

Design of Si-photonic structures to evaluate their radiation hardness dependence on design parameters

This content has been downloaded from IOPscience. Please scroll down to see the full text.

2016 JINST 11 C01040

(<http://iopscience.iop.org/1748-0221/11/01/C01040>)

View [the table of contents for this issue](#), or go to the [journal homepage](#) for more

Download details:

IP Address: 128.141.133.79

This content was downloaded on 09/05/2017 at 16:02

Please note that [terms and conditions apply](#).

You may also be interested in:

[A system-level model for high-speed, radiation-hard optical links in HEP experiments based on silicon Mach-Zehnder modulators](#)

M. Zeiler, S. Detraz, L. Olantera et al.

[New optical technology for low mass intelligent trigger and readout](#)

D Underwood, B Salvachua-Ferrando, R Stanek et al.

[Optical links for detector instrumentation: on-detector multi-wavelength silicon photonic transmitters](#)

D. Karnick, P. Skwierawski, M. Schneider et al.

[Irradiation tests on InP based Mach Zehnder modulator](#)

D Gajanana, M van Beuzekom, M Smit et al.

[Optical frequency comb generation using two cascaded intensity modulators](#)

Lei Shang, Aijun Wen and Guibin Lin

[Thin hybrid pixel assembly with backside compensation layer on ROIC](#)

R. Bates, C. Buttar, T. McMullen et al.

[Irradiation of new optoelectronic components for HL-LHC data transmission links](#)

S Seif El Nasr-Storey, S Detraz, L Olantera et al.

[Integrated optical Mach-Zehnder modulator with a linearized modulation characteristic](#)

Evgenii M Zolotov and R F Tavlykaev

RECEIVED: October 30, 2015

REVISED: November 13, 2015

ACCEPTED: December 7, 2015

PUBLISHED: January 19, 2016

TOPICAL WORKSHOP ON ELECTRONICS FOR PARTICLE PHYSICS 2015,
SEPTEMBER 28TH – OCTOBER 2ND, 2015
LISBON, PORTUGAL

Design of Si-photonic structures to evaluate their radiation hardness dependence on design parameters

M. Zeiler,^{a,1} S. Detraz,^a L. Olantera,^a G. Pezzullo,^a S. Seif El Nasr-Storey,^{a,b} C. Sigaud,^a
C. Soos,^a J. Troska^a and F. Vasey^a

^aEP-ESE Department, CERN,
Route de Meyrin, Geneva, Switzerland

^bSchool of Physics, University of Bristol,
Tyndall Avenue, Bristol, United Kingdom

E-mail: marcel.zeiler@cern.ch

ABSTRACT: Particle detectors for future experiments at the HL-LHC will require new optical data transmitters that can provide high data rates and be resistant against high levels of radiation. Furthermore, new design paths for future optical readout systems for HL-LHC could be opened if there was a possibility to integrate the optical components with their driving electronics and possibly also the silicon particle sensors themselves. All these functionalities could potentially be combined in the silicon photonics technology which currently receives a lot of attention for conventional optical link systems. Silicon photonic test chips were designed in order to assess the suitability of this technology for deployment in high-energy physics experiments. The chips contain custom-designed Mach-Zehnder modulators, pre-designed “building-block” modulators, photodiodes and various other passive test structures. The simulation and design flow of the custom designed Mach-Zehnder modulators and some first measurement results of the chips are presented.

KEYWORDS: Radiation damage to electronic components; Radiation-hard electronics; Optical detector readout concepts

¹Corresponding author.

Contents

1 Motivation	1
2 Technology background	2
2.1 Silicon photonic Mach-Zehnder modulators	2
2.2 Prototype fabrication	4
3 Simulation, design and results	5
3.1 Simulation procedure	5
3.2 Simulation results	5
3.3 Integration into mask file	6
3.4 Measurement results	7
4 Conclusions	7

1 Motivation

The High-Luminosity LHC (HL-LHC) will produce a higher rate of particle collisions compared to that at the Large Hadron Collider (LHC). This entails more stringent requirements on the radiation resistance of the electrical and optical components that will be installed close to the particle interaction points in the HL-LHC. Additionally, components that provide higher data rates will be needed to cope with the increased traffic generated by the growth in measurement data.

The first efforts to identify a solution for this purpose have been launched at CERN in 2013 and 2014 with the Silicon Photonics and Versatile Link PLUS projects. Silicon photonics (SiPh) technology is currently regarded as a promising candidate to address these challenges. SiPh transceivers offer single-channel data rates of 40 Gb/s and above [1, 2] as well as wavelength-multiplexing [3]. This would allow the transmission of more data through a single optical fibre than in current systems and thereby the fibre count in the detectors could be scaled down. SiPh technology also offers the possibility for monolithic [4, 5] or hybrid [6] integration with driving electronics. This would enable a decreased module footprint while at the same time achieving increased chip functionality. Finally, radiation hardness similar to that of silicon particle sensors [7, 8] could be expected. Thus, electro-optic modules could be placed closer to the interaction points and copper wiring could be reduced.

First irradiation test results indeed have shown that SiPh Mach-Zehnder modulators (MZM) suffer almost no degradation in their optical phase modulation performance when exposed to neutron fluences up to $1.0 \cdot 10^{15} \text{ n/cm}^2$ [9, 10]. However, the same MZMs strongly degrade when exposed to ionizing radiation. Their optical phase modulation performance goes down to zero before the highest total ionizing dose (TID) levels expected in HL-LHC (1 MGy) are reached [11]. Therefore, an MZM design with improved resistance against TID damage has to be found [12] before it can

be decided whether the SiPh technology could replace currently installed VCSEL-based (vertical cavity surface emitting laser) optical link systems. More precisely, we aim for an MZM design that is ideally resistant against a neutron fluence of $3.0 \cdot 10^{16} \text{ n/cm}^2$ and a TID of greater than 1 MGy. Devices resistant to those levels could be installed in all locations of the experiments — even in the innermost regions of the tracking detectors. For this purpose, we designed two SiPh chip layouts that include several MZMs in which the design parameters were varied in order to identify the most critical ones with regards to radiation hardness.

This paper presents the electro-optic device simulation methodology, the mask layouts that have been produced and the first test results. Section 2 outlines the operating principle of SiPh MZMs and introduces some background on the fabrication of the prototypes. Section 3 demonstrates the simulation and design work that has been done. Pre-irradiation measurement results obtained from chips fabricated by *imec* are also included. Conclusions are drawn in section 4.

2 Technology background

2.1 Silicon photonic Mach-Zehnder modulators

An MZM is an interferometric modulator that is used for conversion of data streams from the electrical to the optical domain. Incoming light is split equally into two separate modulation arms and an optical path length difference is introduced between them. Depending on this path length difference, both light beams accumulate different phases until they reach the combiner as shown in figure 1. This phase difference produces either constructive or destructive interference at the MZM output. The resulting amplitude modulation is thus achieved by phase modulation in one or both modulation arms. If the two light beams are in-phase when arriving at the combiner, constructive interference occurs and maximum optical power is coupled out of the chip. If there is a non-zero phase shift $\Delta\phi$ between both light beams, the optical power coupled out of the chip depends on that phase shift. In case the phase shift obeys

$$\Delta\phi = m\pi \quad \text{with } m \in \{1, 2, 3, \dots\}, \quad (2.1)$$

complete destructive interference occurs and all the optical power coupled into the chip is radiated away from the waveguides into the surrounding material.

In order to build an MZM in silicon, waveguides have to be patterned into the silicon layer. The light in a silicon waveguide is horizontally confined by sandwiching the silicon layer between

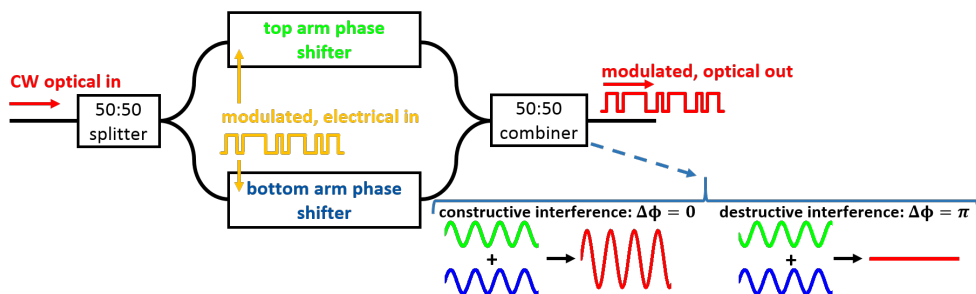


Figure 1. Schematic of the operating principle of an integrated Mach-Zehnder modulator.

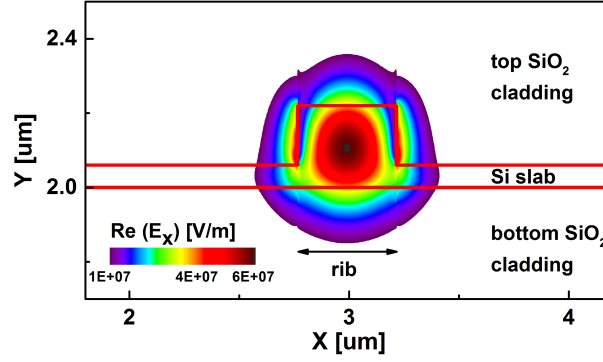


Figure 2. Simulated profile of a guided TE0 mode in a typical silicon waveguide.

two layers of lower refractive index, usually SiO₂. The waveguide is laterally defined by etching away some of the silicon to define a rib. A simulated profile of a guided mode in such a waveguide is shown in figure 2. The phase of the light traveling through such a silicon waveguide can be altered by changing the refractive index n of the waveguide's material. Unlike other materials that show electro-optic effects, the most efficient way to induce changes in the refractive index of silicon is through the Plasma Dispersion Effect [13]. The Plasma Dispersion Effect describes the change in the optical absorption coefficient when carriers are injected into or depleted from a material. Governed by the Kramers-Kronig relations, a change in absorption, i.e. the imaginary part of the complex refractive index, also induces a change in the real part of the complex refractive index. Thus, n can be modified by changing the carrier concentration. A correlation between changes in electron and hole densities, N_e and N_h , respectively, and the refractive index as well as the absorption coefficient α was empirically discovered by Soref and Benett [14]. For light with a wavelength of $\lambda = 1550$ nm, the corresponding equations read

$$\Delta n = -8.8 \cdot 10^{-22} \Delta N_e - 8.5 \cdot 10^{-18} \Delta N_h^{0.8}, \quad (2.2)$$

$$\Delta \alpha = 8.5 \cdot 10^{-18} \Delta N_e + 6.0 \cdot 10^{-18} \Delta N_h. \quad (2.3)$$

Depletion-type modulators, where carriers are swept out of the pn-junction, are most commonly implemented because of their wider modulation bandwidth in comparison to injection type modulators [15]. Figure 3 illustrates the change in the hole density in a typical silicon depletion-type phase shifter with a pn-junction incorporated into the waveguide. Due to the change of the refractive index of silicon, the mode guided in this waveguide will consequently change its effective refractive index n_{eff} . This change Δn_{eff} then translates into a phase shift of

$$\Delta \phi = \frac{2\pi \Delta n_{\text{eff}} L}{\lambda}, \quad (2.4)$$

with L being the length of the phase shifter. The better the overlap between optical mode and depletion zone [17], the higher the phase shift in a modulator arm for a given voltage change ΔV and phase shifter length and the more efficient the phase shifter design.

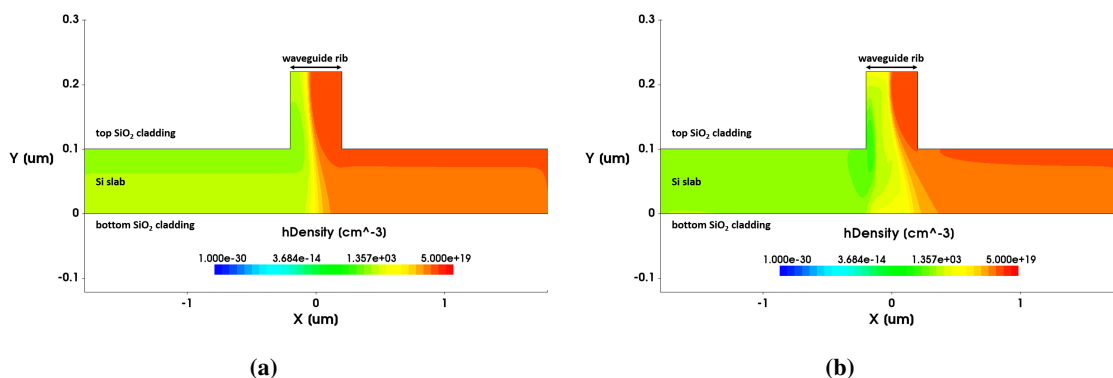


Figure 3. Cross-section of an unbiased (a) and 3V-reverse biased (b) depletion-type phase shifter. The schematic illustrates how holes are swept out of the pn-junction under reverse voltage (after [16]).

2.2 Prototype fabrication

Multi-Project-Wafer (MPW) runs for silicon photonics, offered through the ePIXfab consortium [18], were chosen for the fabrication of our prototypes. In an MPW, the area of a wafer is shared among multiple designs from individual customers. This drastically reduces the fabrication costs for only a few prototypes compared to fabricating unshared wafers. The foundries that realised our chip layouts are *imec* (Belgium) [19] and *CEA-Leti* (France) [20].

In order to satisfy as broad as possible a customer base, all fabrication steps in an MPW are pre-defined and cannot be modified by the customers. As a consequence, the design freedom in an MPW run is constrained. In return, the foundries offer pre-designed devices, so called building blocks, that can be used to create more complex photonic circuits without the need to design every single component from scratch. The design parameters that can be varied in the offered MPWs include: etch depths of waveguide, width of low doping region, length of phase shifter and doping concentrations in waveguide; see figure 4 for parameter explanations.

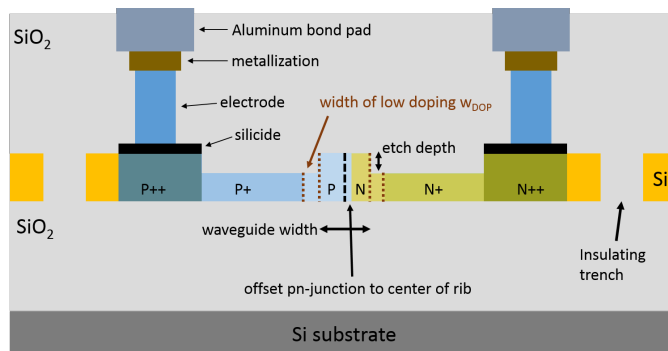


Figure 4. Cross-section through a typical phase shifter.

3 Simulation, design and results

Several MZMs were designed with different parameters, exploiting the few available process variations. To ensure the functionality and optimise the efficiency of the custom designed MZMs, the phase shift vs. voltage characteristic of all potential device designs was simulated. The implementation of the steady-state electro-optical simulations into the available software tools and some results from the simulations and pre-irradiation measurements are presented in this section.

3.1 Simulation procedure

The Synopsys Sentaurus TCAD software [21] was used to simulate the electrical properties of the pn-junctions in silicon under bias. A 2D, cross-sectional phase shifter model for each design parameter set of interest was defined in Sentaurus. The electron and hole densities in the silicon waveguide layer were computed by solving the Poisson and current-continuity equations as a function of an applied bias voltage. The carrier densities were extracted from the device model and converted with the Soref-Benett formulas, eq. (2.2) and (2.3), to a uniform grid of complex refractive indices. The resulting changes in n_{eff} were then computed with a finite-difference mode solver in the OptoDesigner software from Phoenix [22]. The phase shift resulting from a voltage change was finally calculated with eq. (2.4).

3.2 Simulation results

Simulation results were produced for different waveguide etch depths, waveguide rib widths and positions of the pn-junction inside the waveguide for the processes offered by *imec* and *CEA-Leti*. Both foundries offer the same “shallow etch” depths of 70 nm. The “deep etch” depth is 120 nm and 150 nm for *CEA-Leti* and *imec*, respectively. The width of the waveguide was varied between 400 nm and 480 nm. The offset of the pn-junction with respect to the center of the waveguide was varied between -0.3 and 0.2 . It is normalized to the rib width and measured relative to the center of the waveguide. The absolute offset for a rib width of e.g. 400 nm and an offset of -0.2 is thus $-0.2 \cdot 400 \text{ nm} = -80 \text{ nm}$. In this case, the pn-junction is shifted 80 nm away from the center of the waveguide towards the n-doped region. If the offset is positive, it moves towards the p-doped region.

The outcomes of the simulations clearly indicate which parameter set leads to the highest phase shift for both foundries. Example results of the expected phase shift under a reverse bias of 3 V for phase shifters with $L = 4 \text{ mm}$ are shown in figure 5. The largest phase shift, independent of etch depth, can be expected for MZMs where the pn-junction is centered in the waveguide. As the confinement of the optical mode in a deep etch waveguide is better than in a shallow etch waveguide, the overlap with the depletion zone is larger and therefore the phase shift is greater than in shallow etch waveguides. To compensate for this reduced overlap, the rib width of shallow etch waveguides needs to be widened for enhanced phase shift performance. On the contrary, the rib width of deep etch waveguides does not influence the simulated phase shift strongly. Because relatively high phase shifts can be anticipated for both etch depths with a rib width of 450 nm (marked with “X” in figure 5), and to have a common reference design, we decided to take this value for all our custom designed MZMs.

MZMs typically show large losses due to free carrier absorption because of the relatively high doping concentrations in the order of $1 \cdot 10^{17} - 1 \cdot 10^{18} \text{ cm}^{-3}$ in the waveguide. The same simulations

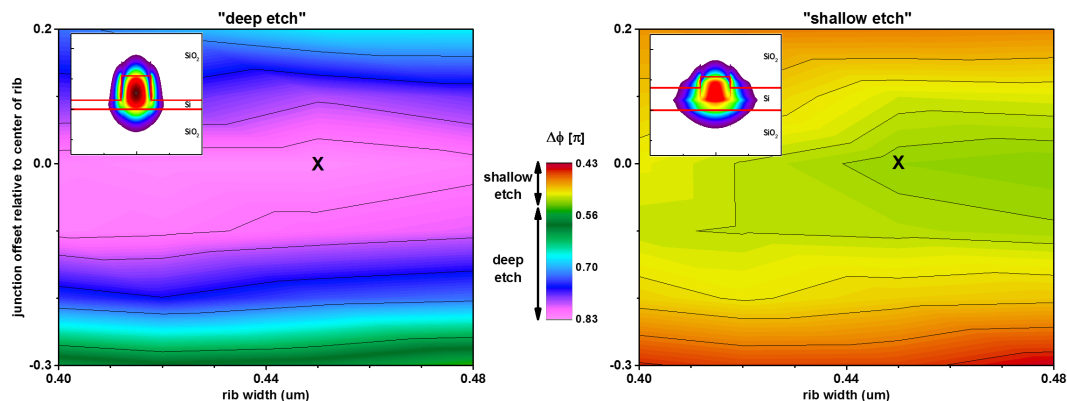


Figure 5. Simulated phase shift for a reverse bias of 3 V and $L = 4$ mm. The insets show the profile of the electric field of the guided TE₀ mode for the two available etch depths.

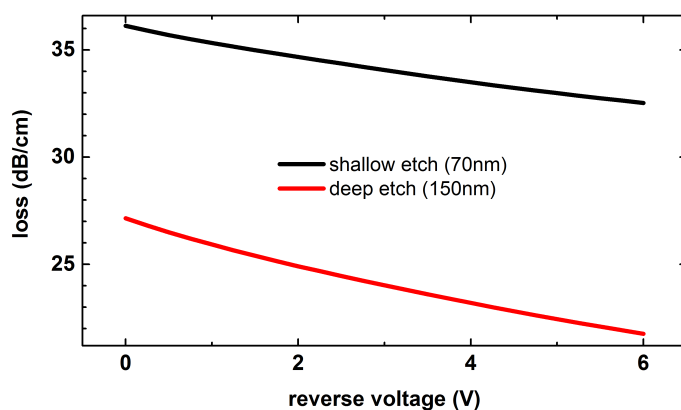


Figure 6. Simulated phase shifter loss under reverse bias for deep and shallow etch waveguides with a rib width of 450 nm and a junction offset of 0.0.

were used to determine optical losses for the design parameter set of choice. The simulations confirm that absorption losses for phase shifters only a few millimeter long are within an acceptable range. Figure 6 shows that deep etch waveguides have losses about 25 % lower than shallow etch waveguides. This stems from the less strongly confined mode in a shallow etch waveguide which extends further laterally into the highly doped regions, and hence experiences more free carrier absorption.

3.3 Integration into mask file

The simulation results were used to define the parameters for custom designed MZMs that were integrated into the two distinct mask layouts for *CEA-Leti* and *imec* as shown in figure 7. Both layouts also contain photodiodes and various passive test structures, e.g. doped and undoped waveguides to assess the change in optical absorption as a function of TID or neutron fluence. Since the *imec* reticle is more than twice as large as the *CEA-Leti* reticle, many more designs with varied parameters are included. The *imec* chips were produced in two different sub-versions, one with the nominal doping concentration and one with a doubled doping concentration around the center of the

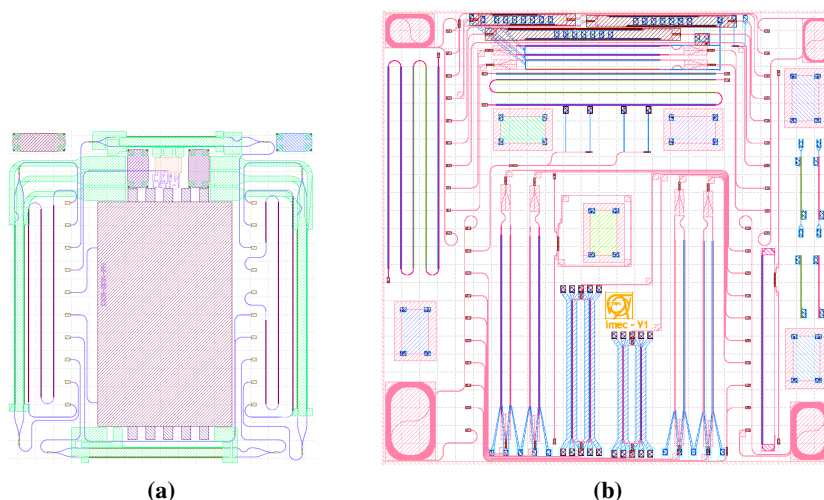


Figure 7. Mask layers of the produced layouts for *CEA-Leti* (a) and *imec* (b) in scale to each other. The size of the *CEA-Leti* reticle is 3.4 mm by 3.7 mm, while the size of the *imec* reticle is 5 mm by 5 mm.

waveguide. The intermediate doping (N+/P+) and the contact doping concentrations (N++/P++) remain the same.

Both layouts also include building block MZMs for referencing. Building block grating couplers and multi-mode interference couplers are used to couple light into/out of the chip and to split/recombine the light in custom designed MZMs, respectively.

3.4 Measurement results

The chips from *imec* have been fabricated and were tested for functionality. The pre-irradiation phase shift of the fabricated chips was determined by coupling light from a superluminescent diode (SLED) into the MZMs and recording the transmission spectra at different bias voltages with an optical spectrum analyzer (figure 8). The results clearly confirm that MZMs realised in deep etch waveguides show larger phase shifts than MZMs realised in shallow etch waveguides. In addition, the good agreement between measured and simulated phase shifts can be regarded as a verification of the implemented simulation model.

4 Conclusions

Custom made silicon photonic components are being investigated as a potential new technology for radiation hard optical links in high-energy physics experiments (HEP). We went through the entire process of chip design, from electro-optical device simulations to mask layout and device testing. Pre-irradiation tests show that the chips from *imec* are fully functional. As soon as the initial testing is complete, some chips will be exposed to x-rays to assess how the design parameters of MZMs affect the phase shift and absorption as a function of ionizing dose.

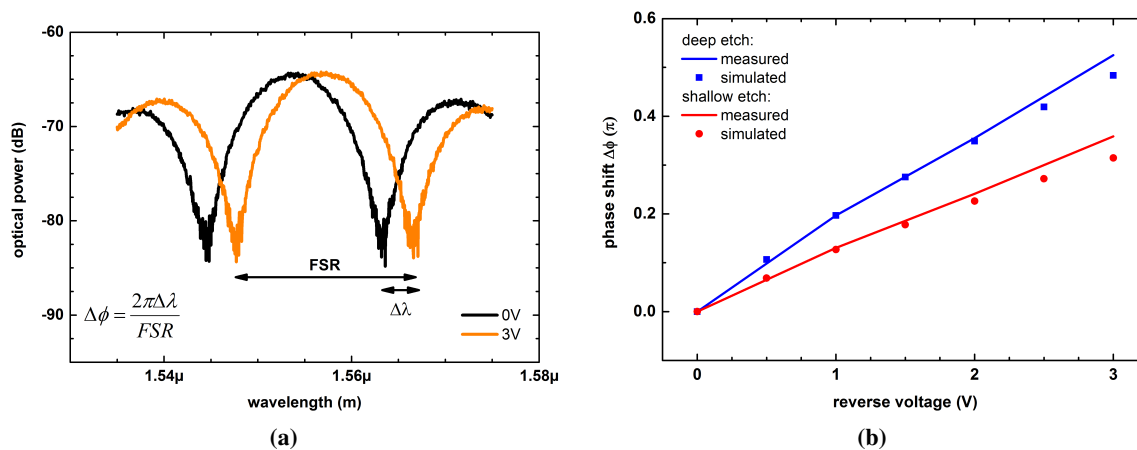


Figure 8. Example spectra of a 1.9 mm-long MZM in *imec*'s shallow etch waveguide (a). The free spectral range (FSR) and the wavelength shift ($\Delta\lambda$) are used to calculate the phase shifts. The resulting phase shift for both etch depths is in good agreement with the one predicted in the simulation (b).

Acknowledgments

Parts of this work have been funded through the ICE-DIP programme. ICE-DIP is a European Industrial Doctorate project funded by the European Commission's 7th Framework programme Marie Curie Actions under grant PITN-GA-2012-316596.

References

- [1] M. Streshinsky, R. Ding, Y. Liu and A. Novack, *Low power 50 Gb/s silicon traveling wave Mach-Zehnder modulator near 1300 nm*, *Optics Express* **21** (2013) 30350.
- [2] F. Y. Gardes and D. J. Thomson, *40 Gb/s silicon photonics modulator for TE and TM polarisations*, *Optics Express* **19** (2011) 11804.
- [3] Y. Chetrit, J. Basak, H. Nguyen, D. Rubin and M. Paniccia, *Wavelength Division Multiplexing Based Photonic Integrated Circuits on Silicon-on-Insulator Platform*, *IEEE J. Sel. Top. Quant. Electron.* **16** (2010) 23.
- [4] M. Webster et al., *An efficient MOS-capacitor based silicon modulator and CMOS drivers for optical transmitters*, in *IEEE 11th Int. Conf. on Group IV Photonics (GFP)* **1** (2014) 1.
- [5] D.M. Gill et al., *Monolithic Travelling-Wave Mach-Zehnder Transmitter with High-Swing Stacked CMOS Driver*, *Conf. on Lasers and Electro-Optics* **1** (2014) 1.
- [6] N. Qi et al., *A 25Gb/s, 520mW, 6.4Vpp Silicon-Photonic Mach-Zehnder Modulator with Distributed Driver in CMOS*, in *Optical Fiber Communication Conference*, Los Angeles, CA, U.S.A., 22–26 March 2015, pg. 1–3.
- [7] G. Casse et al., *Thin Silicon Detectors for Tracking in High Radiation Environments*, *IEEE Nucl. Sci. Symp. Med. Imag. Conf. Rec.* **1** (2012) 1661.
- [8] CERN RD50 collaboration, A. Candelori, *Radiation-hard detectors for very high luminosity colliders*, *Nucl. Instrum. Meth. A* **560** (2006) 103.

- [9] S. Seif El Nasr-Storey et al., *Silicon Photonics for High Energy Physics Data Transmission Applications*, in *IEEE 11th Int. Conf. on Group IV Photonics (GFP)* **1** (2014) 1.
- [10] S.S. El Nasr-Storey et al., *Neutron and X-ray irradiation of silicon based Mach-Zehnder modulators*, *2015 JINST* **10** C03040.
- [11] S. Seif El Nasr-Storey et al., *Effect of Radiation on a Mach-Zehnder Interferometer Silicon Modulator for HL-LHC Data Transmission Applications*, *IEEE Trans. Nucl. Sci.* **62** (2015) 329.
- [12] S. Seif El Nasr-Storey et al., *Modeling TID Effects in Mach-Zehnder Interferometer Silicon Modulator for HL-LHC Data Transmission Applications*, *IEEE Trans. Nucl. Sci.* **62** (2015) 2971.
- [13] J. Basak et al., *Developments in gigascale silicon optical modulators using free carrier dispersion mechanisms*, *Adv. Opt. Technol.* **2008** (2008) 678948.
- [14] R. Soref and B. Bennett, *Electrooptical effects in silicon*, *IEEE J. Quant. Electron.* **23** (1987) 123.
- [15] D. Marris-Morini et al., *Optical modulation by carrier depletion in a silicon PIN diode*, *Optics Express* **14** (2006) 10838.
- [16] D. Marris-Morini et al., *A 40 Gbit/s optical link on a 300-mm silicon platform*, *Optics Express* **22** (2014) 6674.
- [17] H. Xu et al., *High speed silicon Mach-Zehnder modulator based on interleaved PN junctions*, *Optics Express* **20** (2012) 15093.
- [18] *ePIXfab*, <http://www.epixfab.eu/>.
- [19] *imec*, http://www.europractice-ic.com/SiPhotonics_technology_imec_ISIPP25G.php.
- [20] *CEA-Leti*, <http://www-leti.cea.fr/en/How-to-collaborate/Focus-on-Technologies/Integrated-silicon-photonics>.
- [21] Synopsys, *Sentaurus Device*, <http://www.synopsys.com/Tools/TCAD/DeviceSimulation/Pages/SentaurusDevice.aspx>.
- [22] Phoenix, *OptoDesigner 5*, <http://www.phoenixbv.com/product.php?submenu=dfa&subsubmenu=3&prdgrpID=3>.